Computational Study of the Mixed Cooling Effects on the In-Vessel Retention of a Molten Pool in a Nuclear Reactor

Byung Seok, Kim
School of Mechanical Engineering, Kyungpook National University, 1370, Sankyuk-dong, Daegu 702-701, Korea
Kwang Il, Ahn
Integrated Safety Assessment, Korea Atomic Energy Research Institute, 150, Dukjin-dong, Daejon 305-353, Korea
Chang Hyun, Sohn*
School of Mechanical Engineering, Kyungpook National University, 1370, Sankyuk-dong, Daegu 702-701, Korea

The retention of a molten pool vessel cooled by internal vessel reflooding and/or external vessel reactor cavity flooding has been considered as one of severe accident management strategies. The present numerical study investigates the effect of both internal and external vessel mixed cooling on an internally heated molten pool. The molten pool is confined in a hemispherical vessel with reference to the thermal behavior of the vessel wall. In this study, our numerical model used a scaled-down reactor vessel of a KSNP (Korea Standard Nuclear Power) reactor design of 1000 MWe (a Pressurized Water Reactor with a large and dry containment). Well-known temperature-dependent boiling heat transfer curves are applied to the internal and external vessel cooling boundaries. Radiative heat transfer has been considered in the case of dry internal vessel boundary condition. Computational results show that the external cooling vessel boundary conditions have better effectiveness than internal vessel cooling in the retention of the melt pool vessel failure.

Key Words: Nuclear Severe Accidents, In-Vessel Retention (IVR), Internal and External Vessel, Mixed Cooling, Computational Fluid Dynamics (CFD)

Nomenclature

A : Surface area of a hemispherical pool (m^2)
C : Morphology constant
c : Specific heat capacity (J/kg·K)
f : Lliquid fraction of solidifying melt ($0<\Delta H/L<1$)
g : Gravity acceleration vector (m/s^2)
ΔH: Nodal latent heat undergoing phase change ($0<\Delta H<L$) (J/kg)

* Corresponding Author,
E-mail : chsohn@knu.ac.kr
TEL : +82-53-950-5570; **FAX** : +82-53-950-6550
School of Mechanical Engineering, Kyungpook National University, 1370, Sankyuk-dong, Daegu 702-701, Korea. (Manuscript **Received** May 10, 2003; **Revised** March 15, 2004)

H_l : Initial depth of molten liquid relocated in lower plenum (m)
h : Enthalpy (J/kg)
K_p : Permeability
L : Latent heat of fusion (J/kg)
Nu : Nusselt number
p : Pressure (N/m^2)
q'' : Heat flux (W/m^2)
$\bar{q}''$: Surface-averaged heat flux (W/m^2) $\left(=\int_S q'' dA/A\right)$
q''' : Volumetric heat source (W/m^2)
R : Inner radius of the hemispherical cavity (m)
R' : Ratio of the up-to-down heat fluxes
Ra': Modified Rayleigh number based on

q''' $(=\rho^2 cg\beta q''' R^5/\kappa^2\mu)$
T : Temperature (K)
$\mathbf{u}$: Velocity vector (m/s)
V : Volume of a hemispherical pool (m^3)

Greeks

ρ : Liquid density (kg/m^3)
β : Thermal expansion coefficient of liquid (1/K)
ε : Emissivity
κ : Thermal conductivity (W/mK)
θ : Angle along the vessel wall
μ : Dynamic viscosity (kg/m·s)

Sub/superscripts

avg: Average
b : Buoyancy
dn : Downward
e : Electricity
h : Latent heat
l : Liquid
mp : Molten pool
s : Surface
th : Thermal
u : Velocity
up : Upward

1. Introduction

One of the most important issues arising in the analysis of severe core meltdown accidents, is to predict accurately the possibility of IVR (In-Vessel Retention) through the removal of the decay heat generated in the molten corium from the lower head of the RPV (reactor pressure vessel), by either reflooding of the internal vessel or flooding of the reactor cavity. The possibility of IVR depends on heat flux on the inner side of the vessel (between the melt and the wall), the heat transfer on the upper side of the molten pool (between the melt pool and the upper boundary), the heat conductivity of the vessel material and the heat transfer at the outer side of the wall (between the wall and the boiling water). Among these, the downward heat transfer from the molten pool to the peripheral crust region has a direct impact on the conduction heat flux out to the reactor lower head, which, in turn, determines damage to the lower head wall. Various heat transfer mechanisms should be considered when investigating these issues, including the natural convection of a molten pool, the thermal interaction between the molten pool and the vessel wall, the possibility of the internal and external cooling of the reactor walls, and the mechanical behavior of the vessel (Lee and Bankoff, 1998). For a successful IVR, it should be proven that the heat transfer is so efficient that at least part of the RPV wall thickness maintains its structural properties and is able to support the mechanical load that results from both the weight of the corium and the lower head, and from the pressure difference between the inside and the outside of the RPV.

Internal vessel cooling can be made by a mitigating accidental action like a passive internal vessel water injection to cool down molten or particulate debris accumulated in the lower head of the vessel during a late core degradation phase. Internal vessel water injection to cool down the lower head debris bed is still recognized as an important cooling method, but this cooling method creates negative effects such as significant hydrogen generation. In contrast, the external vessel cooling has been regarded as one of the IVR strategies, by keeping the temperature of a significant portion of the RPV lower-head below the wall creep deformation criteria. Intensive research has been performed worldwide on the feasibility of IVR through an external cooling of the reactor lower head as a possible accident management strategy (O'Brien and Hawkes, 1991 ; Park and Dhir, 1992 ; Theofanous et al., 1995 ; Chu, et al., 1997 ; Cheung and Liu, 1999). It has been shown that the small and medium-sized reactor designs could maintain the integrity of the reactor lower-head during a severe core meltdown accident (Theofanous et al., 1995). The efficiency of external vessel cooling should be investigated further to explore the feasibility of corium vessel retention, particularly for reactor vessels with high volumetric heating rates.

However, fewer studies have been performed on the effects of internal and external vessel mixed cooling on RPV thermal behavior. The main

purpose of this paper is to numerically investigate the effects of both internal and external vessel cooling on the retention of an internally heated hemispherical molten pool vessel. In the present analysis, a $1/8^{th}$ linearly scaled-down reactor vessel from the Korean Standard Nuclear Power Plant (KSNP, a PWR of 1000 MWe with a large and dry containment) is utilized as the numerical model. The present study simulates conjugate problems (natural convection with solid-liquid phase change heat transfer in the molten pool and heat conduction in the vessel wall) with internal and external vessel cooling boundary.

2. Scaling Analysis and Assumptions

Figure 1 shows a schematic diagram of the molten pool system and cooling boundary conditions. In the present analysis, it is assumed that the scale-down vessel lower head with an inner radius of 0.25 m is filled with Al_2O_3 melt simulant (with a Prandtl number of 0.68) in place of a molten pool corium pool (with a Prandtl number of 0.5~0.8) (Kang et al., 1998 ; 2000). These geometrical and molten pool conditions have been utilized in the LAVA-4 gap-cooling experiment (Kang et al., 2000) of the SONATA experimental series (Suh et al., 1995).

In a scaled-down reactor vessel, it is necessary to specify an appropriate heat source comparable to a typical reactor case. In order to simulate the real thermal load on the vessel wall, the amount of power density generated in the molten pool

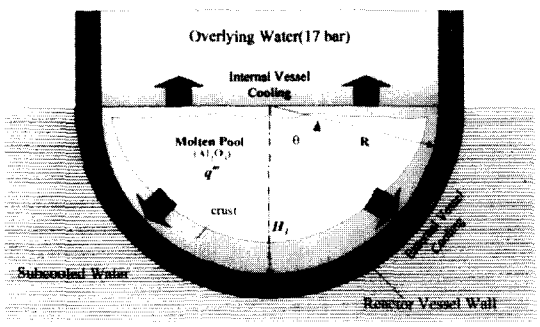

Fig. 1 Schematic of the hemispherical pool and boundary cooling conditions

(via an external heating method such as direct electrical or Joule heating) is determined by equating the downward averaged heat flux ($\bar{q}''_{dn}$, eq. (1)) in the scaled-down vessel to that in a typical reactor. The downward averaged heat flux ($\bar{q}''_{dn}$) corresponding to the decay heat is about 0.6 MW/m^2 for the KSNP design with an electric power of 1000 MW_e (thermal power of 3000 MW_{th}) and with the PRV inner radius of 2.06 m. The internal heat generation can be estimated by the following overall heat balances (eqs. (1)~(3)) that equate heat loss from a hemispherical pool to the both upward and downward surfaces (Theofanous et al., 1997 ; Epstein, 1989).

$$\bar{q}''_{dn}=q''' V_{mp}\{2\pi R^2(1+0.5R')\}^{-1} \quad (1)$$

$$q'''=(A_{up}\bar{q}''_{dn}+A_{dn}\bar{q}''_{dn})/V_{mp},\ V_{mp}=\frac{2}{3}\pi R^3 \quad (2)$$

$$R'=Nu_{up}/Nu_{dn} \quad (3)$$

Here, the ratio of the up-to-down heat fluxes, R', depends on the modified Rayleigh number (Ra') and the strength of natural convection occurring within the molten pool. The decay heat power densities are 1.3 MW/m^3 for $R'=1.0$ and 1.43 MW/m^3 for $R'=1.3$, respectively (Theofanous et al., 1997). The present scaled-down reactor vessel ($R=0.25$ m), with an internal power density of 10.8 MW/m^3 in the case without natural convection ($R'=1.0$), or 11.8 MW/m^3 in the case with natural convection ($R'=1.3$) is required to generate the same heat fluxes as that of the KSNP. In this analysis, we utilized a lower power density of 10 MW/m^3 corresponding to the lower bound of internal power density. This heat source is characterized by the modified Rayleigh number of 6.75×10^{10} in the present scaled-down geometry and this value is much lower than real corium expected in the core meltdown accident ($Ra=10^{14}\sim10^{17}$). Since the modified Ra number is the only representative dimensionless group of natural convection heat transfer with heat source, the present value of the modified Rayleigh number corresponds to a laminar-to-turbulence transient regime of natural convection flow under a given Prandtl number (0.68). No special turbulence

models need to be used up to a Ra number of 10^{12} (Nourgaliev et al., 1997).

In order to describe molten pool thermal behavior, the following assumptions are incorporated in the present numerical model.

(1) The liquid molten pool material is subjected to a single species with a uniform heat source.

(2) The flow of the Newtonian fluid is axisymmetric, laminar and incompressible.

(3) The material properties are constant during the whole transient time and the Boussinesq approximation is applicable.

(4) An enthalpy formulation for the energy equation can be to account for phase changes.

(5) The crust is assumed to be homogeneous without gap cooling through porous media.

Based on the aforementioned conditions, the initial and geometric data are summarized in Table 1. Thermophysical properties for the melt pool simulant and the vessel wall are given in Table 2.

The current model predictions has been validated by considering a zero heat source for which reliable experimental data are available for a LAVA reactor. The current model predictions are compared with LAVA-6 tests having less gap cooling than other experiments with the outside

Table 1 Initial and boundary conditions

Lower Head Geometric Conditions	Melt simulant :	Al_2O_3
	Lower Head Inner Radius :	0.25 m
	Vessel wall thickness :	0.025 m
Molten Pool Initial Conditions		
- System pressure (bar)	17	
- Pool depth or Aspect ratio (H_l/R)	1.0 (fully filled with Al_2O_3 in the lower plenum)	
- Initial melt pool temperature (K)	2500 (180 K superheated)	
- Melt pool heat source (MW/m^3)	10 ($=S_{q'''}$)	
	($Ra'=6.75\times10^{10}$)	
	(cf. $Ra'\approx10^{14}\sim10^{17}$ for oxidic core melts)	
- Prandtl number of melt	0.68 (cf. $Pr\approx0.6-0.8$ for oxidic core melts)	
- Vessel wall temperature (K)	427 (50 K subcooling at 17 bar)	
Boundary Cooling Conditions		
- Melt pool overlying water (K)	477 (saturation temperature at 17 bar)	
- Ex-vessel water temperature (K)	323 (50 K subcooling at 1 bar)	
- Ex-vessel heat transfer coefficient (dry case)	Constant heat transfer coefficient (50 W/m^2K)	

Table 2 Thermophysical properties used in the present analysis

Thermophysical parameters	Melt simulant : Al_2O_3	Vessel wall : Stainless steel
Melting temperature (K)	2320	1800
Latent heat of fusion (J/kg)	1.12×10^6	2.5×10^5
Specific heat (J/kg·K)	1230	540
Thermal conductivity (W/m·K)	9.0	35
Density (kg/m)	3751	8000
Dynamic viscosity (kg/m·s)	5.0×10^{-3}	—
Thermal diffusivity (m^2/s)	1.95×10^{-6}	—
Thermal expansion coefficient (1/K)	1.65×10^{-5}	—
Thermal radiation emissivity	0.6	0.6
Morphology constant	1.0×10^6	

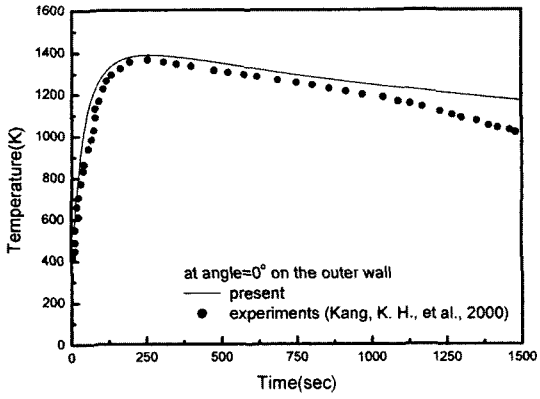

Fig. 2 Molten pool average temperature

wall in the lower plenum of vessel begin cooled by radiation after 250 sec. The results of the comparison made are as indicated in the Fig. 2. The computed results are in good agreement with those obtained experimentally.

3. Numerical Techniques and Boundary Conditions

3.1 Numerical techniques

A computational program has been developed and this program has the capabilities of analyzing (1) laminar natural convection of a single component fluid with volumetric heat generation, (2) liquid-solid phase change in the fluid, and (3) heat conduction in a hemispherical vessel wall containing the fluid. In the validation studies, this program was well verified through the analysis of the partial solidification of a molten pool with/without volumetric heat sources for rectangular laminar flow regime of a molten pool (Kim et al., 2000; Ahn et al., 2000).

The computational boundaries are treated as radiation, convection, and pool-boiling heat-removal. Under the above assumptions, the conservation equations are given as follows.

Conservation of mass

$$\nabla\cdot\mathbf{u}=0 \tag{4}$$

Conservation of momentum

$$\rho_{ref}\left[\frac{\partial\mathbf{u}}{\partial t}+(\mathbf{u}\cdot\nabla)\mathbf{u}\right] =-\nabla p+\nabla\cdot(\mu\nabla\mathbf{u})+S_b+S_u \tag{5}$$

Conservation of energy

$$\rho_{ref}\left[\frac{\partial h}{\partial t}+(\mathbf{u}\cdot\nabla)h\right] =\nabla\cdot[\kappa\nabla(h/c)]+S_{q'''}+S_h \tag{6}$$

Heat conduction in the vessel wall

$$\rho_{ref}\left(\frac{\partial h}{\partial t}\right)=\nabla\cdot[\kappa\nabla(h/c)] \tag{7}$$

Source terms

$$S_b=-\rho_{ref}g\beta(h-h_{ref})/c \tag{8}$$

$$S_u=-\frac{\mu}{K_p}\mathbf{u} \tag{9}$$

$$S_h=-\rho_{ref}L\left[\frac{\partial f}{\partial t}+(\mathbf{u}\cdot\nabla)f\right] \tag{10}$$

$$S_{q'''}=const \tag{11}$$

Here, the buoyancy source term, S_b, accounts for the natural convection effects of the molten pool. The velocity source terms, S_u, are used to suppress or initiate the velocity components as the liquid material undergoes a phase change from a liquid state to a solid state or vice versa.

$$K_p=\frac{f^3}{C(1-f)^2} \tag{12}$$

where K_p is the permeability and C is constant dependent on the morphology of the porous medium (Voller, 1987). f is liquid fraction defined as $\Delta H/L$. The energy source term, S_h, is used to account for the effect of solidification. The first term in the square brackets, $\partial f/\partial t$ describes the energy released from the liquid phase when solidification is made and the second term accounts for the convective effects due to the presence of a mushy region (if it exists). Finally, the volumetric heat source term is given as $S_{q'''}$ as shown in table 1.

In order to evaluate the flow and enthalpy fields, the above set of coupled partial differential equations is discretized by the body-fitted non-orthogonal grids (Choi et al., 1993; Ferziger and Peric, 1996) using a finite volume approach with collocated arrangements of variables. The discretized equations are solved iteratively using the strongly implicit procedure (Stone, 1968) and

the SIMPLEC algorithm (Van and Raithby, 1984). The second order Euler backward implicit time step method is employed for constructing the discretization equations for unsteady flow and enthalpy. The QUICK scheme (Hayase et al., 1992) with deferred correction (Khosla and Rubin, 1974) is utilized to discretize the convective term of the momentum equation. For the method undergoing a phase change a Darcy source technique (Voller and Swaminathan, 1991) is used.

Grid dependency is checked with three different grid sizes (42×42, 72×72 and 92×92) and 72×72 is employed for computing the discrete values of the velocities and the enthalpy in the domain. To calculate the transient phenomena on the molten pool and vessel thermal behavior, a constant time step of 0.05 sec was applied. It was confirmed that a smaller time step did not change the accuracy. Convergence criteria was $1\times10^{-4}\%$ of the total mass present in the hemispherical cavity and then the absolute value of the energy balance error (the density product the surface integral of new latent heat subtracted from the old value) dropped below $1\times10^{-3}\%$.

3.2 Initial and Boundary cooling conditions

In the LAVA experiment, the initial temperature of the molten pool is assumed to be 2500 K (180 K superheat is the number correct), and the initial temperature of the vessel wall is given the same 427 K (50 K subcooling at 17 bar) (Kang et al., 2000).

The upper surface of the melt pool may be cooled by the overlying water (i.e., wet condition) or subjected to a dry atmosphere (i.e., dry condition). A radiative heat transfer formula is utilized for the dry case and a boiling heat transfer is assigned to the wet case. For the wet case, the Rohsenow correlation (Rohsenow and Choi, 1961) and modified Bromley correlation (Collier, 1981) are employed for a nucleate boiling regime and for a film boiling regime, respectively. Also, critical and minimum heat fluxes are calculated using the Zuber correlation (Churchill and Churchill, 1975). In a transition boiling regime, a logarithmic interpolation between the CHF (critical heat flux) and the minimum film boiling heat flux are used to determine the heat flux at that temperature. In addition, radiation heat transfer between a melt pool surface and an

Table 3 Upward pool boiling correlations

Correlations	Correlations according to regime (upward)
Nucleate boiling regime	$\left[\frac{C_{pl}(T_{surf}-T_{sat})}{h_{fg}}\right]=C_{sf}\left[\frac{q''_{nb}}{\mu h_{fg}}\left(\frac{\sigma}{g(\rho_l-\rho_v)}\right)^{1/2}\right]^n \mathrm{Pr}^m$ *Rohsenow*
Film boiling regime	$q''_{film}=0.943[\rho_v(\rho_l-\rho_v)gk_v^3(h_{fg}+1/2c_{pv}\Delta T)\mu_v L_c]^{1/4}\Delta T^{0.75}$ *Modified Bromley*
Minimum film boiling regime	$q''_{mfilm}=0.09\rho_v h_{fg}[\sigma(\rho_l-\rho v)g/\rho_l^2]^{1/4}[\rho_l/(\rho_l+\rho_v)]^{1/2}$ *Zuber*

Table 4 Downward pool boiling correlations

Correlations	Correlations according to regime (Downward)
Subcooled regime	$h_L=0.135[1.414+21.76(T_{wo}-T_L)^{1/6}]^2$, $(323\le T_{wo}\le409\ \mathrm{K})$ *Churchill and Churchill*
Nucleate boiling regime	$h_L=0.55\frac{(T_{wo}-T_{sat})^3}{T_{wo}-T_L}$, $(409\le T_{wo}\le633\ \mathrm{K})$ Experimental results of Dhir
Transient boiling regime	$h_L=532.5\left[\frac{553}{T_{wo}-T_{sat}}\right]^{5.393}$, $(633\le T_{wo}\le926\ \mathrm{K})$ Experimental results of Dhir

overlying water pool is added during stable film and transition boiling. The details of the above correlations are presented in Table 3. The feedback effect of thermal hydraulic conditions due to sustained steam generation and associated system pressurization is neglected. Analyses are not considered for the venting of a steam/water mixture on the top, and the dynamic behavior of the two-phase natural circulation flow.

The exterior of the vessel may be submerged in water (i.e., wet condition) or subjected to the atmosphere (i.e., dry condition). A constant natural heat transfer coefficient is utilized for the dry case and boiling heat transfer correlation for the wet case. For the dry case, a heat transfer coefficient of 50 W/m^2K (Bejan, 1993) is taken due to natural convection for surrounding air temperature of 323 K at 1 bar. Also, the radiation effect outside the exterior wall through air is added between the exterior wall and the surrounding atmosphere. For the wet condition, the present model utilizes the average single phase natural convection heat transfer coefficient for a submerged hemisphere which is obtained from the correlation suggested by Churchill and Churchill for subcooled water (Churchill and Churchill, 1975). Also, the heat transfer coefficients in nucleate and transitional boiling are obtained by two correlations based on the experimental Dhir's results (Dhir, 1978). The present cooling model is only applied to the pool boiling condition, but bubble behavior along the curved surface (i.e., two-phase hydrodynamics) is not taken into account to obtain heat transfer at the surface.

4. Numerical Results and Discussions

Computational calculations were carried out for up to 2500 seconds to get transient local heat fluxes and temperatures at the vessel wall for three typical azimuthal angles (0°, 50°, 80°).

In order to gain further insight on the effectiveness of internal and external vessel mixed cooling on the corium vessel retention, the present numerical simulations are performed for each of the following four different boundary conditions:

(Case 1) no water cooling in internal and external vessel (dry in-vessel and dry ex-vessel);

(Case 2) water cooling in internal vessel and no water cooling in external vessel (wet in-vessel and dry ex-vessel);

(Case 3) no water cooling in internal vessel with water cooling in external vessel (dry in-vessel and wet ex-vessel);

(Case 4) water cooling in internal and external vessels (wet in-vessel and wet ex-vessel);

4.1 Molten pool thermal behavior

Figure 2 shows the total volume-averaged temperatures of the molten pool for four different cases, which are governed by the energy balance between the heat generation rate within the molten pool and the heat loss rate through the boundaries. If the rate of heat generation in the molten pool exceeds the heat loss, the molten pool will remain in liquid phase near its upper surface. Also, the initial temperature of the interior wall vessel is much lower than the solidifying temperature of the molten pool and consequently a crust will immediately form on the inner wall of the vessel that is in contact with the molten corium.

In Case 1, the average temperature of the molten pool increases monotonously and reach 2937 K at 2500 seconds. In the dry case, the heat from the upper surface of the molten pool is transported by radiation. In Case 2, the temperature increases up to a maximum temperature of 2780 K at about 1400 seconds and thereafter it remains saturated up to a temperature of 2772 K, which is much higher than the melting temperature of the vessel. Dry external conditions such as Cases 1 and 2 give rise to increasing average temperatures, so the average temperature cannot be lowered without external cooling. Even if there is water cooling in the internal vessel as in Case 2, the average temperature increases. The results of Case 2 are mainly due to the fact that the wet internal upper boundary heat transfer condition generates film boiling condition rather than a nucleate boiling one. If the superheat of

molten pool is in the region of nucleate boiling, the internal vessel cooling will be highly effective in removing internal heat from the molten pool.

When external vessel cooling conditions such as in Cases 3 and 4, are imposed, the molten pool average temperature slowly decreases until it reaches a quasi-steady temperature of 1800 K. The result of Case 3 shows that external vessel cooling is a highly effective cooling boundary condition than is the internal cooling boundary condition. However, despite additional cooling in internal vessel such as in Case 4, mixed cooling boundary conditions give slight effects, compared to external vessel cooling conditions.

Figures 3(a) and (b) show the average upward and downward heat fluxes for each of the four cases. The average downward heat fluxes for Cases 3 and 4 in Figure 3(b) are much higher than those in Cases 1 and 2 in Figure 3(a). This means that the downward cooling in Cases 3 and 4 removes heat more than upward cooling in Cases 1 and 2, because the downward heat flux is under the nucleate boiling regime. Downward cooling conditions in Cases 3 and 4 present a peak heat flux value approximately after 50 seconds. After this time, downward heat fluxes decrease gradually due to heat transfer resistance by crust formation.

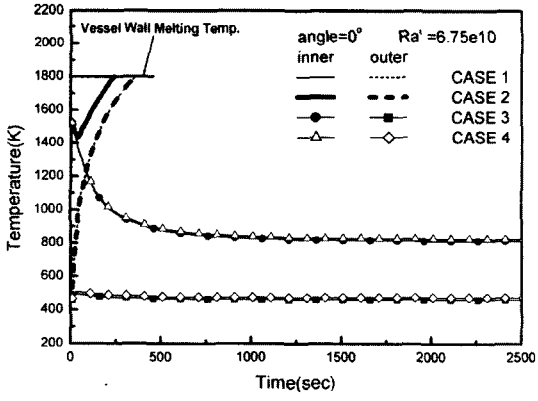

(a) Case 1 and 2

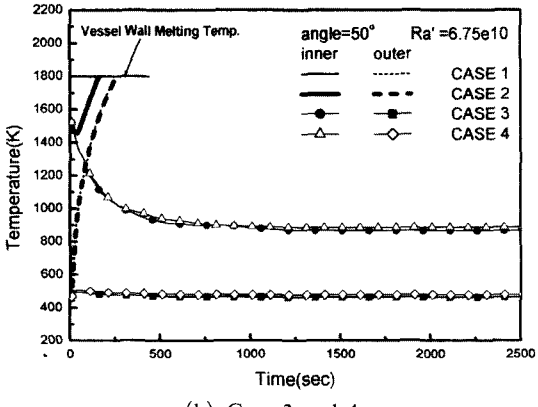

(b) Case 3 and 4

Fig. 3 Comparison of upward and downward with the average heat fluxes

4.3 Temperature transient with angular position

Figures 4(a) to 4(c) show the variation of local temperatures for three different angular positions (0°, 50°, 80°) at the inner and outer walls of the hemispherical vessel. Case 1 and Case 2 reach melting temperature of vessel at 240 seconds and 160 seconds for 0° and 50°, respectively. And, temperature at 80° begins to exceed melting temperature after 90 seconds. There is a trend of increasing heat flux with increasing azimuthal angle because of buoyancy force effects. As shown in Figure 4, Case 3 and Case 4 are also similar to Case 1 and Case 2 in view of the inner and outer wall temperatures increasing. Although direct comparison with experiments cannot be made, the above results are consistent with Theofanous's experiments, which were implemented under wet external cooling conditions (Theofanous, 1997).

The temperature differences between the inner and outer wall for Cases 3 and 4 are much larger than that for Case 1 and Case 2. In spite of in-vessel cooling conditions such as Case 2, the entire vessel wall temperatures exceeded the melting point of the vessel (1800 K) after about 90 seconds. The entire vessel wall is maintained far below its melting temperature over the whole transient time in the cases of wet external vessel cooling conditions.

Figures 5 to 7 show velocity vectors and temperature contours for four cooling boundary conditions. As shown in figure 5 of the dry case of the external vessel, it can be seen that the wall of the vessel begins to melt at around 200

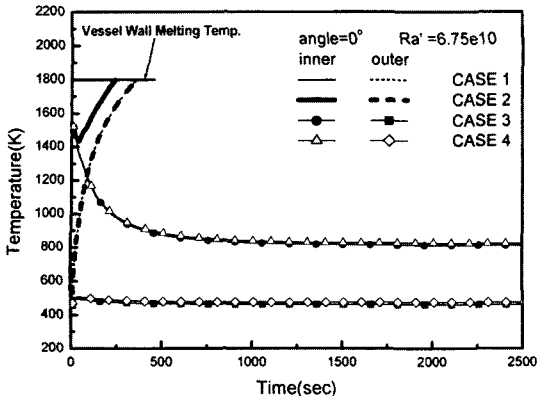

Fig. 4(a) Vessel wall temperature at angular position 0° : inner and outer wall

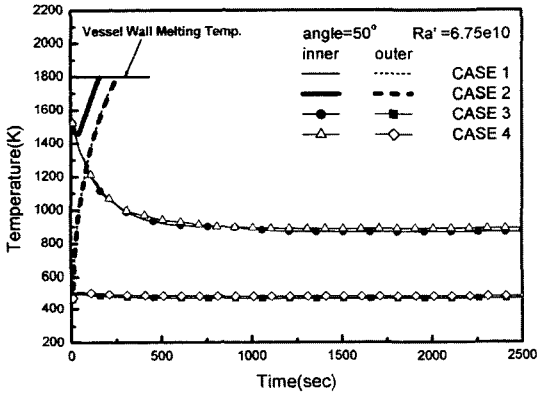

Fig. 4(b) Vessel wall temperature at angular position 50° : inner and outer wall

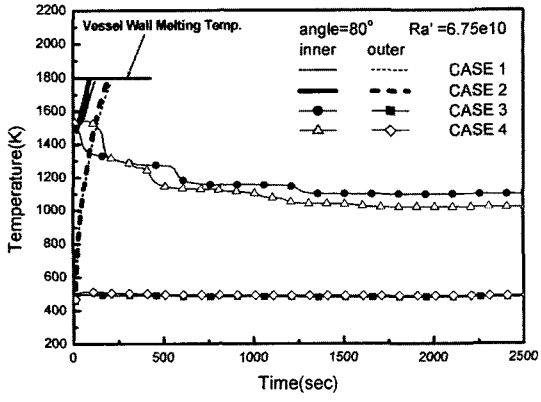

Fig. 4(c) Vessel wall temperature at angular position 80° : inner and outer wall

seconds. As time increases, the molten portion

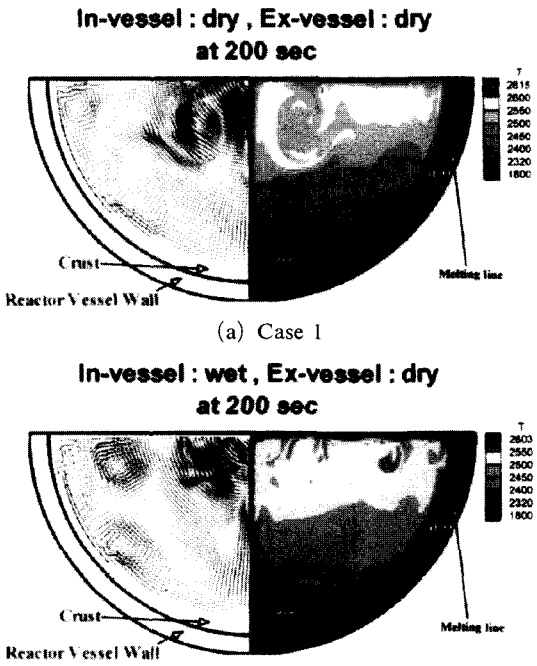

(a) Case 1

(b) Case 2

Fig. 5 Velocity vectors and temperature contours for Case 1 and Case 2

will be larger and larger in the dry external vessel condition. Figure 6 shows the formation of a crust at the upper surface by wet boundary conditions on the internal vessel, which generate film boiling cooling conditions on the upper surface and then reduce the heat transfer rate. Near the upper boundary region, the crust formation of Case 4 (i.e. part of the invisible velocity vectors) is thicker than that of Case 3, because of the lower temperature as shown in Figure 4(c). As seen at 2500 seconds (quasi-steady), internal wet cooling conditions have a little role in heat removal in comparison to Case 3, so the conduction heat transfer through the crust does not contribute to heat removal. Cases 3 and 4 show stronger cooling effects in contrast to Cases 1 and 2 in view of vessel failure retention. Accordingly, this means that external cooling is more effective than internal cooling. This is why external cooling methods with highly effective nucleate boiling make heat transfer enhanced and consequently make the crust formed near the wall.

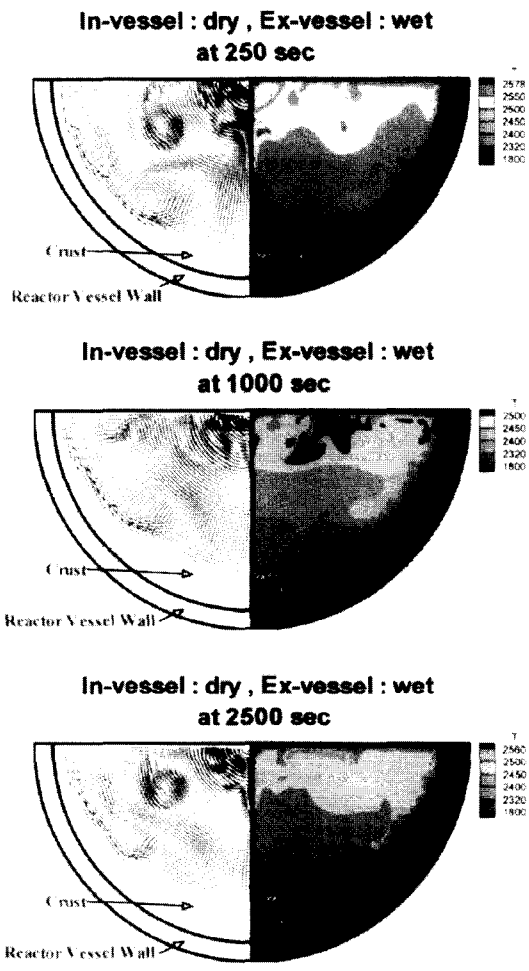

Fig. 6 Velocity vectors and temperature contours with time-varying crust thickness : Case 3

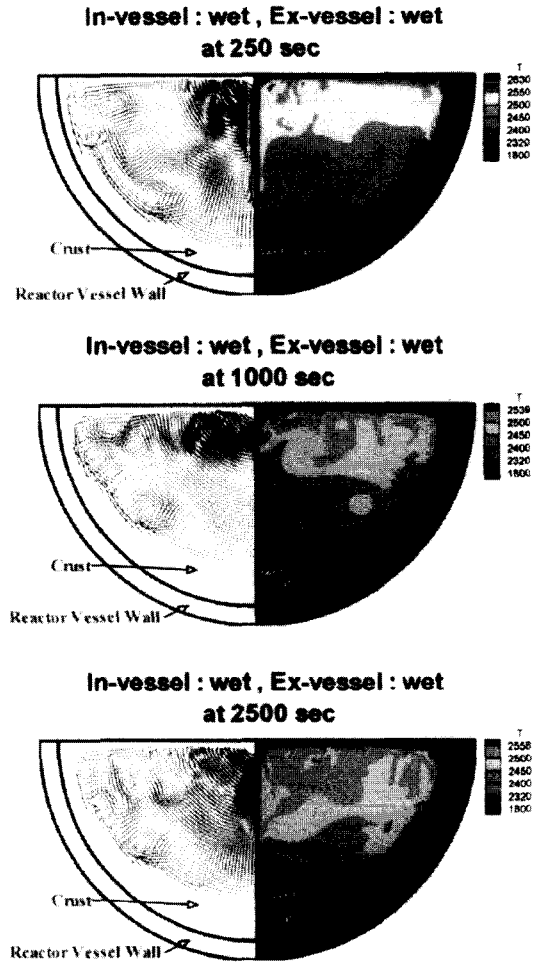

Fig. 7 Velocity vectors and temperature contours with time-varying crust thickness : Case 4

5. Concluding Remarks

The effect of internal and external vessel mixed cooling on the retention of an internally heated molten pool in a scaled-down reactor has been analyzed. Based on the present configuration of the molten pool and cooling boundaries, the time-varying heat flux distributions and the vessel wall temperature distributions have been obtained through a numerical simulation. These results show that downward heat removal by nucleate boiling is substantially more effective than upward heat transfer film boiling added to radiation. Vessel temperature remained far below its vessel melting temperature over the whole transient time in the cases of the wet external vessel cooling, which was subjected to subcooled nucleate boiling with very high heat flux. However, wet internal cooling with dry external condition resulted in temperatures above the melting temperature of the vessel.

The wet external vessel cooling condition is a more effective than the wet internal vessel cooling condition in reactor retention during a severe nuclear accident.

Acknowledgment

This study was carried out under the Nuclear

R&D Program planned by the Korean Ministry of Science and Technology (MOST) and partially supported by the Brain Korea 21 project in 2003.

References

Ahn, K. I., et al., 2000, "Numerical Analysis of the Heat Transfer Characteristics of a Heat Generating Melt Pool Confined in a Hemispherical Cavity with the MELTPOOL Code," *2nd Japan-Korea Symposium on Nuclear Thermal Hydraulics and Safety (NTHAS-2)*, Fukuoka, Japan, pp. 610~617.

Bejan, A., 1993, *Heat Transfer*, 2nd Ed., Wiley, New York.

Cheung, F. B. and Liu, Y. C., 1999, "Effects of Thermal Insulation on External Cooling of Reactor Vessels under Severe Accident Conditions," NURETH-9, CD-ROM publication, California, USA.

Choi, S. K., et al., 1993, "The Choice of Cell Face Velocities in the Three Dimensional Incompressible Flow Calculations on Nonorthogonal Grids," *KSME International Journal*, Vol 6, pp. 154~161.

Chu, T. Y., et al., 1997, "Ex-vessel Boiling Experiments : Laboratory and Reactor-Scale Testing of the Flooded Cavity Concept for In-vessel Retention, Part II : Reactor-scale boiling experiments of the flooded cavity concept for in-vessel core retention," *Nuclear Engineering and Design*, Vol. 169, pp. 89~99.

Churchill, S. W. and Churchill, R. U., 1975, "A Comprehensive Correlating Equation for Heat and Component Transfer by Free Convection," *Journal of AIChE*, Vol. 21, pp. 604~606.

Collier, J. G., 1981, *Convective Boiling and Condensation*, 2nd Ed., McGraw-Hill, New York.

Dhir, V. K., 1978, "Study of Transitional Boiling Heat Fluxes from Spheres Subjected to Forced Vertical Flow," *Intl. Conf. on Heat Transfer*, Toronto, Canada.

Epstein, M. and Fauske, H. K., 1989, "The Three Mile Island Unit 2 Core Relocation-Heat Transfer and Mechanism," *Nuclear Technology*, Vol. 87, pp. 1021~1035.

Ferziger, J. H. and Peric, M., 1996, *Computational Methods for Fluid Dynamics*, Springer-Verlag, Berlin, Germany.

Hayase, T., et al., 1992, "A Consistently Formulated QUICK Scheme for Fast and Stable Convergence Using Finite-Volume Iterative Calculation Procedures," *J. Computational Physics*, Vol. 98, pp. 108~118.

Kang, K. H., et al., 1998, "Review on Experimental Studies for the In-Vessel Corium Retention Research," *KAERI/TR-1032/98.*

Kang, K. H., et al., 2000, "Experimental Investigations on the effects of Water Subcooling for the In-Vessel Debris Coolability In the LAVA Experiment," *NTHAS2 : 2nd. Japan-Korea Symposium on Nuclear Thermal Hydraulics and Safety*, Fukuoka, Japan, pp. 596~603.

Khosla, P. K. and Rubin, S. G., 1974, "A diagonally Dominant Second-Order Accurate Implicit Scheme, Computers Fluids," Vol. 2, pp. 207~209.

Kim, B. S., et al., 2000, "A Computational Model for the Analysis of Heat Transfer Characteristics in Liquid Metal Layer under a Solidification Process : MELTPOOL," *Proceedings of 8th Intl. Conf. on Nuclear Engineering*, ASME/JSME/SFEN, Baltimore, MD, USA.

Lee, S. C. and Bankoff, S. G. ., 1998, "A Comparison of Predictive Models for the Onset of Significant Void at Low Pressures in Forced-Convection Subcooled Boiling," *KSME International Journal*, Vol 12, pp. 504~513.

Nourgaliev, R. R., et al., 1997, "Effect of Fluid Number on Heat Transfer Characteristics in Internally Heated Liquid Pools with Raleigh Numbers up to 1012," *Nuclear Engineering and Design*, Vol. 169, pp. 165~184.

O'Brien, J. E. and Hawkes, G. L., 1991, "Thermal Analysis of a Reactor Lower Head with Core Relocation and External Boiling Heat Transfer," *AIChE Symposium Series*, Vol. 87.

Park, H. J. and Dhir, V. K., 1992, "Effect of Outside Cooling on the Thermal Behavior of a Pressurized Water Reactor Vessel Lower Head," *Nuclear Technology*, Vol. 100, pp. 331~346.

Rohsenow, W. M. and Choi, H., 1961, *Heat, Mass and Momentum Transfer*, Prentice-Hall,

Englewood Cliffs, NJ.

Stone, H. L., 1968, "Iterative Solution of Implicit Approximations of Multidimensional Partial Difference Equations," *SIAM J. Numer. Anal.*, Vol. 5, pp. 330~558.

Suh, K. Y. and Park, K. C., 1995, "SONATA-IV : Simulation of Naturally Arrested Thermal Attack in Vessel," *Proc. Int. Conf. on PSA Methodology and Applications*, Seoul, Korea, pp. 26~30.

Theofanous, T. G., et al., 1997, "In-vessel Coolability and Retention of a Core Melt," *Nuclear Engineering and Design*, Vol. 169, pp. 1~48.

Theofanous, T. G., et al., 1997, "Special Issue on In-vessel Retention," *Nuclear Engineering and Design*, Vol. 169, pp. 1~206.

Van Doormaal, J. P. and Raithby, G. D., 1984, "Enhancements of the SIMPLE Method for Predicting Incompressible Fluid Flows," *Numerical Heat Transfer*, Vol. 7, pp. 147~163.

Voller, V. R. and Prakash, C., 1987, "A Fixed Grid Numerical Modelling Methodology for Convection-Diffusion Mushy Region Phase-Change Problems," *Int. Journal of Heat and Mass Transfer*, Vol. 30, pp. 1709~1719.

Voller, V. R. and Swaminathan, C. R., 1991, "General Source-Based Method for Solidification Phase Change," *Numerical Heat Transfer, Part B*, Vol. 19, pp. 175~189.